Spin Excitations in a Fermi Gas of Atoms

B. DeMarco* and D. S. Jin†

JILA, National Institute of Standards and Technology and University of Colorado, Boulder, Colorado 80309

(Received 30 August 2001; published 11 January 2002)

We have experimentally investigated a spin excitation in a quantum degenerate Fermi gas of atoms. In the hydrodynamic regime the damping time of the collective excitation is used to probe the quantum behavior of the gas. At temperatures below the Fermi temperature we measure up to a factor of 2 reduction in the excitation damping time compared to the classical expectation. In addition, we observe a strong excitation energy dependence for this quantum statistical effect.

DOI: 10.1103/PhysRevLett.88.040405 PACS numbers: 05.30.Fk

Studies of elementary excitations have proven to be an effective tool for investigating the dynamics of dilute, ultracold atomic gases [1]. These systems are fertile testing grounds for many-body quantum theory because the interactions, which arise via collisions between the constituent atoms, can be described from first principles. For fermions there are essentially no interactions in a single-component gas at ultralow temperature. However, an interacting Fermi gas was recently realized using magnetically trapped ^{40}K atoms in two different spin states [2]. The collective excitation behavior for such a mixed spin component Fermi gas is rich and has been investigated theoretically in both the collisionless and hydrodynamic regimes [3–8]. Studies of spin excitations may also serve to expose the onset of a superfluid phase in the Fermi gas [8–10]. In the work presented here, we use a dipole ("slosh") spin excitation in the hydrodynamic regime to probe a Fermi gas of magnetically trapped ^{40}K atoms. This type of excitation, which was previously shown to be sensitive to interactions [11], is shown here to probe quantum statistical effects in dynamics of the Fermi gas.

The production of an interacting Fermi gas of atoms follows our previous experimental procedure [2,12]. Fermionic ^{40}K atoms are magnetically trapped in two spin states (the $m_f = 9/2$ and $m_f = 7/2$ Zeeman states in the $f = 9/2$ hyperfine ground state) in order to permit the s-wave collisions necessary for evaporative cooling to ultralow temperature. As in all experiments with atomic Fermi gases [12–14], two components are required because collisions between identical fermions are forbidden by symmetry at the temperatures of interest. The interactions therefore arise in the gas from collisions between, but not within, the $m_f = 9/2$ and $m_f = 7/2$ components.

In the magnetic trap, the $m_f = 9/2$ and $m_f = 7/2$ components have slightly different single-particle harmonic oscillator frequencies because of a small disparity in their magnetic moments. This small difference in the bare harmonic oscillator frequencies determines the collision rate necessary to reach the hydrodynamic regime for the type of excitation used in this work [11]. For the measurements described in this Letter, the single-particle oscillator frequencies for the $m_f = 9/2$ component were 256 Hz radially and 19.8 Hz axially [15]. The bare trap frequencies for the $m_f = 7/2$ component are reduced from these values by a factor of $\sqrt{7/9}$.

The excitation studies used a gas of 0.7×10^6 to 3.3×10^6 atoms, in a nearly equal mixture of the two-spin states, cooled to a temperature between 0.24 and 2.0 μK. A dipole, or slosh, oscillation was excited by shifting the trap center for approximately half of an axial period (28 ms) along the axial trap direction as described in Ref. [11]. The resulting motion of the gas, involving center-of-mass oscillation of each component about the trap center, was allowed to evolve in the magnetic trap. Before imaging the gas, the magnetic trap was quickly turned off so that the gas expanded ballistically for 16 ms. During the expansion, the two components were spatially separated by a magnetic field gradient [2,16]. The number, temperature, and center of mass of both components were determined from independent fits to each absorption image taken after expansion. The dynamics of the dipole excitation were mapped out by varying the evolution time in the magnetic trap before release.

The center-of-mass positions of both components were recorded as a function of time and then fit simultaneously to exponentially damped harmonic motion in order to extract the normal mode frequency and damping rate. The two normal modes of the system transform from independent oscillations at the bare trap frequencies in the collisionless regime to in-phase and out-of-phase oscillations in the hydrodynamic regime [11]. Because the out-of-phase mode is overdamped in the hydrodynamic regime, we probed only the "in-phase" mode. However, the motion of the two components is not perfectly in phase due to the difference in the bare trap frequencies for the two spin states. The mode we observe consists primarily of sloshing of the entire gas along the axial trap direction, but also includes a small amount of relative motion between the two spin components. This relative motion provides sensitivity to interactions and gives rise to an axial magnetization in the cloud's center-of-mass frame that oscillates in space and time.

This type of excitation is reminiscent of the well-known spin waves in quantum fluid and solid state systems, and

is similar to the spin waves observed in spin-polarized hydrogen gases [17]. The existence of a spin excitation requires a spin dependent interaction. In our case, spin dependent forces arise from the magnetic trapping potential and also from the quantum nature of the collisions. Even at temperatures well above the degenerate regime for bosons or fermions, the quantum statistics distinguishes collisions between atoms in the same internal state and those between atoms in different internal states. Spin then serves as a marker that distinguishes two different Fermi gases. One might expect that collisions between atoms in different spin states would strongly damp a spin excitation, which must involve relative motion of the two-spin components. However, the nearly in-phase normal mode that we study here has a relatively small amplitude of the variation in magnetization.

Before probing the quantum Fermi gas, we explored the spin excitation in the nondegenerate regime [11]. While the frequency of the spin excitation was nearly independent of the collision rate $\Gamma_{\rm coll}$ in the gas, the damping time depended linearly on $\Gamma_{\rm coll}$. In Fig. 1 we plot the measured exponential damping time τ for the spin excitation vs the average collision rate per particle, $\Gamma_{\rm coll}$. The collision rate per particle is defined by $\Gamma_{\rm coll} = 2n\sigma v/(N_{9/2} + N_{7/2})$, where the density overlap $n = \int n_{9/2}(\mathbf{r}) n_{7/2}(\mathbf{r})\, d^3\mathbf{r}$, the total number of atoms $N_{9/2} + N_{7/2}$, and the mean relative speed v for a collision between a $m_f = 9/2$ and $m_f = 7/2$ atom are determined from Gaussian fits to the absorption images. The s-wave cross section is given by $\sigma = 4\pi a^2$, where the triplet scattering length for ^{40}K is $a = 169 a_0$ [18] (a_0 is the Bohr radius). The data in Fig. 1 are taken in the nondegenerate regime, with the temperature T of the gas greater than the Fermi temperature T_F for either spin-state component. The Fermi temperature depends on the number of atoms N and the radial and axial harmonic oscillator frequencies ω_r and ω_z through $T_F = \hbar(6\omega_r^2\omega_z N)^{1/3}/k_b$ [19].

As expected, the damping time increases linearly with the collision rate in the hydrodynamic regime [20]. The increase in damping time, or equivalently reduction in damping rate, is due to the fact that the higher collision rate more firmly establishes the collective excitation. The data in Fig. 1 are fit to a classical kinetic model [11], where the spin components are treated as two harmonic oscillators coupled by collisional viscous damping. The data agree well with the model, which includes a scaling constant on the collision rate axis as the only fit parameter. The best fit value for this scaling factor is within our estimated 50% uncertainty in determining the number of atoms.

The quantum nature of the gas is revealed through changes in the excitation dynamics as the gas is cooled below T_F. The damping time of the dipole oscillation is measured for an equal mixture of $m_f = 9/2$ and $m_f = 7/2$ atoms as the temperature of the gas is varied through forced evaporative cooling. The emergence of quantum behavior below T_F is observed by comparing the measured damping time τ to the classical prediction $\tau_{\rm class}$ in the hydrodynamic regime. The measured spin excitation damping time is shown in Fig. 2. The classical prediction is determined by the value of $\Gamma_{\rm coll}$ inferred from the measured n, v and $N_{9/2} + N_{7/2}$ and the fit shown in Fig. 1.

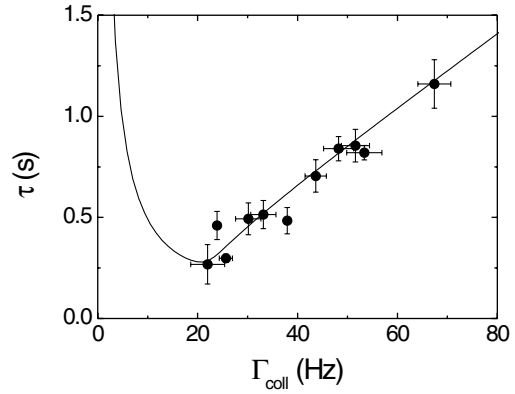

FIG. 1. Damping time of the spin excitation. The exponential damping time τ of the nearly in-phase normal mode is plotted versus the collision rate per particle, $\Gamma_{\rm coll}$. A fit of the data to a classical kinetic model is shown by the solid line. The data shown here are taken in the nondegenerate regime $T/T_F > 1$, and with sufficiently high $\Gamma_{\rm coll}$ to be in the regime of hydrodynamic behavior. The vertical error bars in τ represent the uncertainty from the fits to the center-of-mass motion of the gas, while the horizontal error bars represent variation in $\Gamma_{\rm coll}$ during the oscillation measurement.

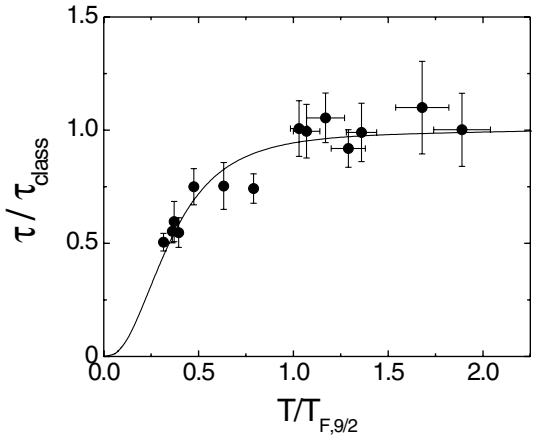

FIG. 2. Effect of quantum degeneracy on the spin excitation damping time. At low T/T_F the measured damping time τ is reduced compared to the classical expectation $\tau_{\rm class}$. The classical expectation $\tau_{\rm class}$ is obtained from the measured collision rate per particle using the fit shown in Fig. 1. The y-axis error bars in this figure and in Fig. 3 include the uncertainties from the fit to the center-of-mass motion, the variation in $\Gamma_{\rm coll}$ during the oscillation measurement, and the fit from Fig. 1. Variation in the temperature during the oscillation measurement is represented by the error bars for $T/T_{F,9/2}$. The data agree well with the theoretical prediction from a quantum kinetic calculation (solid line) of the effect of Pauli blocking on the collision rate.

At low T/T_F we observe that the damping time decreases significantly compared to the classical expectation. This change in the damping arises from a quantum statistical suppression of collisions. In the degenerate Fermi gas low energy quantum states have an occupancy approaching one. This fact combined with the Pauli exclusion principle suppresses the elastic collision rate through a reduction of allowed final states. As seen in Fig. 1, lowering $\Gamma_{\rm coll}$ in the hydrodynamic regime results in a shorter damping time (or equivalently a higher damping rate). Thus by reducing $\Gamma_{\rm coll}$, Pauli blocking hinders the ability of the collective excitation to propagate in the quantum regime. Ultimately, in the zero temperature limit one expects the gas to reach the collisionless and zero-sound regime.

The data in Fig. 2 are compared with the prediction of a quantum kinetic calculation of the $\Gamma_{\rm coll}$ suppression due to Pauli blocking [21], shown by the solid line. The calculation includes the difference in trap frequencies for the $m_f = 9/2$ and $m_f = 7/2$ components and assumes an equal mixture of atoms in the two spin states. For comparison with the measurements, we have plotted the calculated quantum collision rate normalized by the collision rate calculated without Pauli blocking. The nearly factor of 2 reduction in τ (compared to the classical result that neglects Pauli blocking) observed at our lowest T/T_F agrees with the theory.

Pauli blocking of collisions was seen previously in measurements of rethermalization rates in the two-component Fermi gas [2]. Although both the data in Fig. 2 and the previous results can be understood in terms of the very general quantum effect of Pauli blocking, it is important to note that the two experiments probe very different dynamics. In fact, the sign of the measured effect in the two experiments is opposite. The measured rethermalization time increased in the quantum regime, while the measured damping time shown in Fig. 2 decreases in the quantum regime.

The damping rate for the collective excitation also exhibits a strong amplitude dependence in the quantum regime. The dependence of the exponential damping time on the center-of-mass oscillation amplitude A is shown in Fig. 3. The slosh excitation amplitude A is compared to the axial rms size $\sigma_{\rm rms}$ of the $m_f = 9/2$ component. The quantity $(A/\sigma_{\rm rms})^2$, measured after expansion, is proportional to the ratio of the slosh excitation energy to the internal kinetic energy per particle. Data in Fig. 3 were taken with a gas at $T/T_{F,9/2} = 0.4$ and one at $T/T_{F,9/2} = 1.2$, corresponding to the quantum and classical regimes. For the nondegenerate gas we observe no nonlinearity and the damping time is independent of the excitation amplitude over a wide range of excitation energy. In contrast, in the quantum regime we observe a strong amplitude dependence to the damping time. In order to minimize the impact of this nonlinearity the data with $T/T_F < 1$ in Fig. 2 were taken with $(A/\sigma_{\rm rms})^2 < 0.01$.

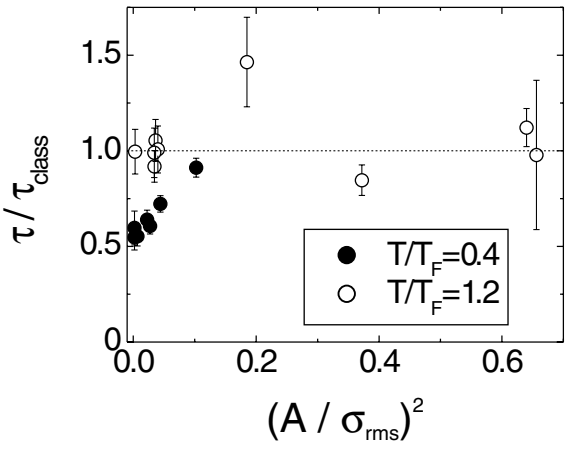

FIG. 3. Nonlinear excitation dynamics. Data for a nondegenerate gas at $T/T_F = 1.2$ are compared to data for a gas in the quantum regime at $T/T_F = 0.4$. For the high temperature data the measured damping time τ matches the classical expectation (dotted line) $\tau_{\rm class}$ over a wide range of excitation amplitude A. In the quantum regime, however, the Pauli blocking effect on τ is strongly reduced as the relative amplitude $A/\sigma_{\rm rms}$ increases.

The observed nonlinearity presumably comes from the energy dependence of the Pauli blocking effect on collisions. A large excitation amplitude increases the average collision energy, and therefore reduces the impact of Pauli blocking. For example, a collision in which an atom gains an energy which is very small compared to the Fermi energy, $E_F = k_b T_F$, will be strongly suppressed in a quantum degenerate gas. Conversely, a collision in which an atom gains an energy that is larger than E_F will not be suppressed at all. We find that the effect of Pauli blocking on τ is significantly reduced for relatively small slosh amplitude. This nonlinear behavior could provide a probe of the Fermi sea structure through the energy dependence of Pauli blocking. Future work along these lines would require a quantitative model for comparison with the observed effect.

In conclusion, we have used a collective spin excitation in the hydrodynamic regime to probe the interplay between interactions and quantum statistics in a Fermi gas of atoms. We measure an increased damping rate compared to the classical expectation at low temperature, and observe nonlinear behavior in the quantum regime. The behavior seen here for spin excitations is general to any two-component Fermi gas and could in principle be observed for a two-isotope gas. If future experiments are able to cool a Fermi gas of atoms to even lower T/T_F, studies similar to those presented here could be used to explore the crossover from hydrodynamic to collisionless behavior due to Pauli blocking in the degenerate gas. Excitation dynamics could also be used to investigate the predicted phase transition to a Cooper-paired superfluid state in a two-component Fermi gas of atoms [8–10].

This work is supported by the National Science Foundation, the Office of Naval Research, and the National

Institute of Standards and Technology. The authors would like to express their appreciation for useful discussions with C. E. Wieman and E. A. Cornell and for work by S. B. Papp.

*Present address: Time and Frequency Division, National Institute of Standards and Technology.

†Qunatum Physics Division, National Institute of Standards and Technology.

[1] F. Dalfovo, S. Giorgini, L. P. Pitaevskii, and S. Stringari, Rev. Mod. Phys. **71**, 463 (1999).

[2] B. DeMarco, S. B. Papp, and D. S. Jin, Phys. Rev. Lett. **86**, 5409 (2001).

[3] L. Vichi and S. Stringari, Phys. Rev. A **60**, 4734 (1999).

[4] G. M. Bruun and C. W. Clark, Phys. Rev. Lett. **83**, 5415 (1999).

[5] M. Amoruso, I. Meccoli, A. Minguzzi, and M. P. Tosi, Eur. Phys. J. D **8**, 361 (2000).

[6] L. Vichi, J. Low Temp. Phys. **121**, 177 (2000).

[7] G. M. Bruun and C. W. Clark, Phys. Rev. A **61**, 061601(R) (2000).

[8] A. Minguzzi and M. P. Tosi, Phys. Rev. A **63**, 023609 (2001).

[9] M. A. Baranov and D. S. Petrov, Phys. Rev. A **62**, 041601 (2000).

[10] G. M. Bruun and C. W. Clark, J. Phys. B **33**, 3953 (2000).

[11] S. D. Gensemer and D. S. Jin, Phys. Rev. Lett. **87**, 173201 (2001).

[12] B. DeMarco and D. S. Jin, Science **285**, 1703 (1999).

[13] A. G. Truscott *et al.,* Science **291**, 2570 (2001).

[14] F. Schreck *et al.,* Phys. Rev. Lett. **87**, 080403 (2001).

[15] Two of the lowest Γ_{coll} data points in Fig. 1 were taken using a weaker trapping potential (135 Hz radial frequency and 19.8 axial frequency for an $m_f = 9/2$ atom).

[16] D. M. Stamper-Kurn *et al.,* Phys. Rev. Lett. **80**, 2027 (1998).

[17] See, for example, B. R. Johnson, J. S. Denker, N. Bigelow, L. P. Levy, J. H. Freed, and D. M. Lee, Phys. Rev. Lett. **52**, 1508 (1984); N. P. Bigelow, J. H. Freed, and D. M. Lee, Phys. Rev. Lett. **63**, 1609 (1989).

[18] H. Wang *et al.,* Phys. Rev. A **62**, 052704 (2000).

[19] D. A. Butts and D. S. Rokhsar, Phys. Rev. A **55**, 4346 (1997).

[20] P. Nozieres and D. Pines, *The Theory of Quantum Liquids* (Perseus Books, Cambridge, 1966).

[21] M. J. Holland, B. DeMarco, and D. S. Jin, Phys. Rev. A **61**, 053610 (2000).